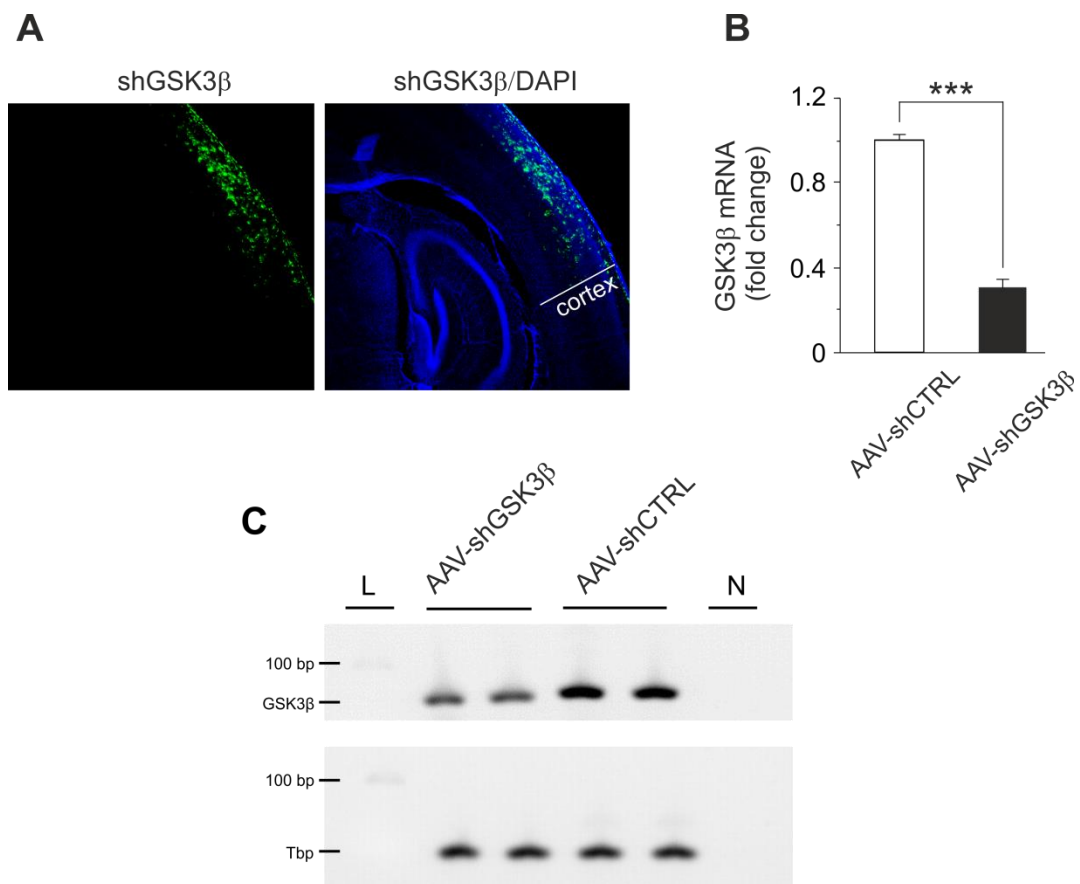
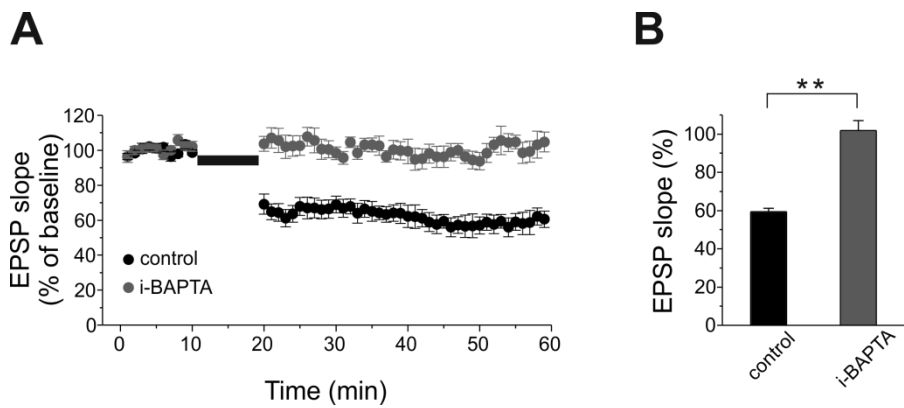


**Supplementary Figure 1. tLTD dependence on the number of APs in the induction protocol.**

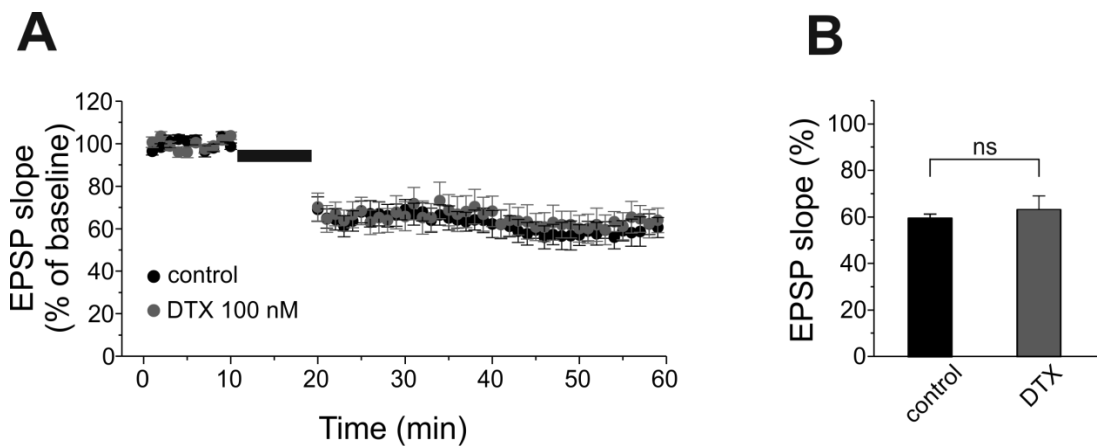
**(A)** Average time course of EPSP slope, normalized to baseline values, during tLTD experiments in which a single AP or a burst of three APs (at 100 Hz) was utilized in the induction protocol. Inset depict the pairing protocol. The last AP preceded the onset of EPSP by  $\Delta t = -10$  ms. Note that tLTD magnitude was correlated only weakly with the number of APs preceding the EPSP. **(B)** Bar graph comparing the average EPSP amplitude measured during the last 5 min recording expressed as a percentage of the baseline slope (100%) under the experimental conditions showed in A (burst protocol:  $n = 10$  from 5 mice; canonical protocol:  $n = 9$  from 5 mice).



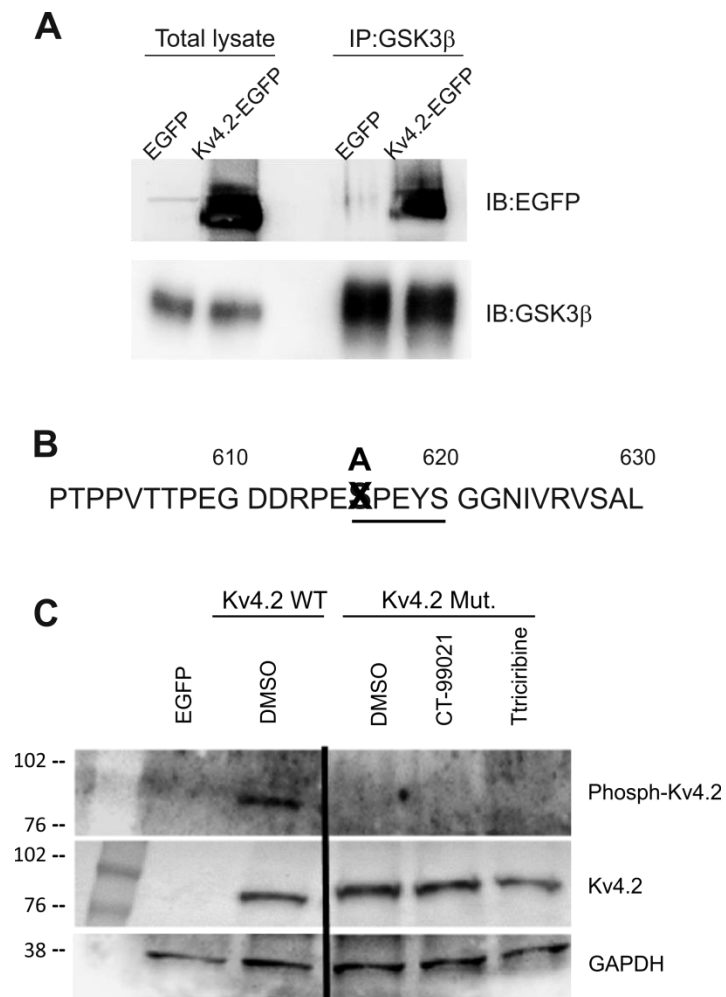
**Supplementary Figure 2. GSK3β shRNA vector validation.** (A) Representative images showing viral vector localization (EGFP immunofluorescence) in the somatosensory cortex (left). EGFP/DAPI staining merge is also shown (right). (B) *In vivo* validation of GSK3β mRNA knockdown in pyramidal neurons by single cell reverse transcription quantitative real-time PCR. Bar graph shows the fold change of GSK3β mRNA normalized to the housekeeping Hprt in control (AAV-shCTRL-GFP) and knocked down (AAV-shGSK3β-GFP) pyramidal somatosensory neurons. Values are expressed as means ± SEM. (*n* = 7 cells per group; **total number of mice: 10**). \*\*\**p*<0.001. (C) Representative Sybr-safe precast agarose gel shows RT-qPCR products of the expected size for GSK3β (72 bp) and Tbp (65 bp) from siRNA GSK3β (Lanes 2 and 3) and Scramble (Lanes 4 and 5) single cell neurons. Two microliters of RT-PCR negative control, add to TaqMan Mix, was used for RT-qPCR negative control (N). Lane 1 represents DNA ladder (L).



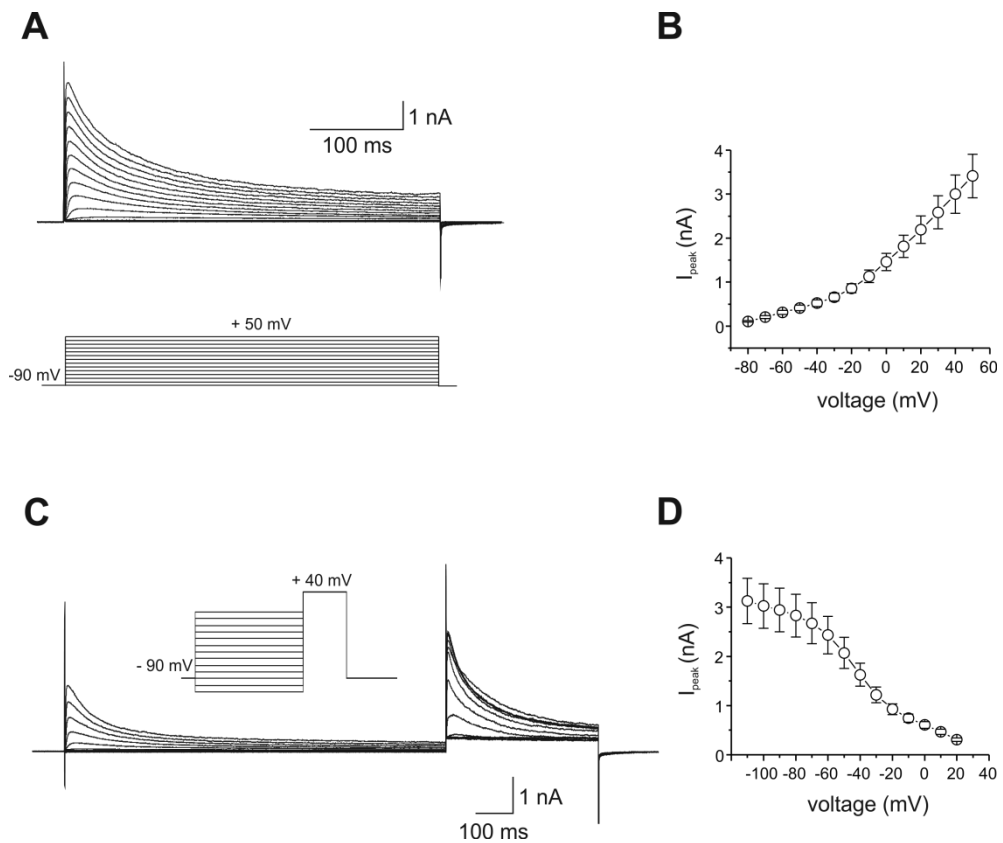
**Supplementary Figure 3. Postsynaptic  $\text{Ca}^{2+}$ -dependency of tLTD.** (A) Average time course of EPSP slope, normalized to baseline values, during tLTD experiments in which BAPTA (10 mM) was intracellularly perfused through the patch-pipette (10 mM; gray circle;  $n = 8$  cells from 4 mice). For comparison, control tLTD is also shown (black circle). (B) Bar graph comparing the average EPSP slope under the experimental conditions showed in A.



**Supplementary Figure 4. Dendrotoxin, a selective Kv1 channel inhibitor, does not affect tLTD.** (A) Average time course of EPSP slope showing that slice treatment with 100 nM DTX does not affect tLTD (gray circle;  $n = 8$  cells from 4 mice). For comparison, control tLTD is also shown (black circle,  $n = 10$  cells from 5 mice). (B) Bar graph comparing the average EPSP slope in the experimental conditions showed in A.



**Supplementary Figure 5. Kv4.2 is bound and phosphorylated by GSK3 $\beta$  in HEK293. In HEK293 cells expressing the mutant Kv4.2<sup>S616A</sup> the phosphorylation of Ser-616 was completely lost.** (A) HEK293 cells expressing either the Kv4.2-EGFP or the EGFP empty vectors were immunoprecipitated (IP) with an antibody against GSK3 $\beta$ . Blots were probed (IB) with antibodies against GSK3 $\beta$  or EFGP. (B) Primary sequence of the C-terminal domain of Kv4.2 channels in which the aminoacid Ser-616 was substituted with the amino acid alanine. (C) Representative blots of total cell lysate from HEK293 cells transfected either with Kv4.2-WT or empty vector (EGFP) or mutated Kv4.2 plasmids probed with anti-phospho-Ser-616 (upper panel) or total Kv4.2 (lower panel) antibodies. Note the absence of phospho-Ser-616 immunoreactivity, in all the experimental conditions, in cells transfected with mutated Kv4.2.



**Supplementary Figure 6. Voltage-dependence of activation and inactivation of transient Kv4.2-induced K<sup>+</sup> currents in HEK293 cells.** (A) Current traces evoked in HEK293 cells expressing KV4.2 by depolarizing steps to potentials between -80 and +50 mV with 10 mV increment from an holding potential of -80 mV. (B) Averaged I-V relationship obtained from 22 recordings. (C) Current traces evoked by test depolarization to +40 mV after 1 s pre-pulse to potentials between -110 and +20 mV with 10 mV increment. (D) Voltage-dependence of steady-state inactivation.